5198–5207 *Nucleic Acids Research, 2017, Vol. 45, No. 9* *Published online 21 February 2017*
doi: 10.1093/nar/gkx130

Highly efficient biallelic genome editing of human ES/iPS cells using a CRISPR/Cas9 or TALEN system

Kazuo Takayama[1,2,3,4], Keisuke Igai[1], Yasuko Hagihara[1], Rina Hashimoto[5], Morifumi Hanawa[1], Tetsushi Sakuma[6], Masashi Tachibana[1], Fuminori Sakurai[1,5,7], Takashi Yamamoto[6] and Hiroyuki Mizuguchi[1,4,5,8,*]

[1]Laboratory of Biochemistry and Molecular Biology, Graduate School of Pharmaceutical Sciences, Osaka University, Osaka 565–0871, Japan, [2]PRESTO, Japan Science and Technology Agency, Saitama 332-0012, Japan, [3]K-CONNEX, Kyoto University, Kyoto 606–8302, Japan, [4]Laboratory of Hepatocyte Regulation, National Institute of Biomedical Innovation, Health and Nutrition, Osaka 567-0085, Japan, [5]Laboratory of Biochemistry and Molecular Biology, School of Pharmaceutical Sciences, Osaka University, Osaka 565-0871, Japan, [6]Department of Mathematical and Life Sciences, Graduate School of Science, Hiroshima University, Hiroshima 739-8526, Japan, [7]Laboratory of Regulatory Sciences for Oligonucleotide Therapeutics, Clinical Drug Development Project, Graduate School of Pharmaceutical Sciences, Osaka University Osaka 565-0871, Japan and [8]Global Center for Medical Engineering and Informatics, Osaka University, Osaka 565-0871, Japan

Received July 22, 2016; Revised February 12, 2017; Editorial Decision February 13, 2017; Accepted February 15, 2017

ABSTRACT

Genome editing research of human ES/iPS cells has been accelerated by clustered regularly interspaced short palindromic repeats/CRISPR-associated 9 (CRISPR/Cas9) and transcription activator-like effector nucleases (TALEN) technologies. However, the efficiency of biallelic genetic engineering in transcriptionally inactive genes is still low, unlike that in transcriptionally active genes. To enhance the biallelic homologous recombination efficiency in human ES/iPS cells, we performed screenings of accessorial genes and compounds. We found that RAD51 overexpression and valproic acid treatment enhanced biallelic-targeting efficiency in human ES/iPS cells regardless of the transcriptional activity of the targeted locus. Importantly, RAD51 overexpression and valproic acid treatment synergistically increased the biallelic homologous recombination efficiency. Our findings would facilitate genome editing study using human ES/iPS cells.

INTRODUCTION

Genome editing of human ES/iPS cells has been limited by technical difficulties that result in a low efficiency of homologous recombination (HR) in human ES/iPS cells. Recently, many researchers have demonstrated that genome editing technologies, such as zinc finger nucleases, transcription activator-like effector nucleases (TALEN) and clustered regularly interspaced short palindromic repeats/CRISPR-associated 9 (CRISPR/Cas9) systems, could enhance the HR and non-homologous end joining (NHEJ) efficiency in human ES/iPS cells by inducing highly specific DNA double-strand breaks (DSB) at the targeted position of the genome (1–6). However, the HR efficiency in human ES/iPS cells is largely dependent on the target locus. Some studies have reported that homozygous targeted clones were almost impossible to obtain (7–9). Hockemeyer *et al*. have shown that human ES/iPS cells were biallelically targeted by using zinc finger nucleases with an efficiency of 2–11% for a transcriptionally active gene, *adeno-associated virus integration site 1* (*AAVS1*), but 0% for transcriptionally inactive gene, *Pituitary homeobox 3* (7). Hockemeyer *et al*. also showed that human ES/iPS cells were biallelically targeted by using TALEN with efficiencies of 9.3–33% for *AAVS1*, but 0–4.1% for *Pituitary homeobox 3* (8). Recently, Yu *et al*. showed that small molecules could enhance CRISPR/Cas9-mediated HR efficiency in human and mouse ES/iPS cells, but the HR efficiency of human ES/iPS cells in the transcriptionally inactive gene, *Alpha smooth muscle actin 2*, was only 1% (9). Chu *et al*. have also reported that CRISPR/Cas9-mediated HR efficiency could be increased by suppressing the NHEJ pathway, but they did not examine whether their method could be also applied to transcriptionally inactive genes (10).

In this study, we tried to develop a method for highly efficient biallelic-targeted gene editing regardless of the transcriptional activity (or chromatin folding) of the targeted locus. To enhance the biallelic HR efficiency in human ES/iPS

*To whom correspondence should be addressed. Tel: +81 6 6879 8185; Fax: +81 6 6879 8186; Email: mizuguch@phs.osaka-u.ac.jp

cells, we performed screenings of accessorial genes and compounds.

MATERIALS AND METHODS

RAD51-Expressing plasmid

The cDNA of the human RAD51 gene (NM_001164269) was amplified by PCR, and then inserted into pBSKII, resulting in pBSKII-RAD51. The human RAD51 gene was inserted into pHMCA5 (11), which contains the CMV enhancer/β-actin promoter with the β-actin intron promoter (CA promoter, kindly gifted from Dr Junichi Miyazaki (Osaka University)), resulting in pHMCA-RAD51. The *Escherichia coli* β-galactosidase (LacZ)-expressing plasmid, pHMCA-LacZ, was constructed previously (11). The primers used for human RAD51 gene cloning are shown below.

Human RAD51 for: 5′-agaTCTAGAgctaatggcaatgcagatgcagct-3′

Human RAD51 rev: 5′-aacGCGGCCGCtcagtctttggcatctcccact-3′

Small-Molecule compound library

The Screenwell Epigenetics library (Enzo Life Sciences) was used in this study. This Screenwell Epigenetics library contains 43 compounds with defined activity against enzymes which carry out epigenetic modification of lysine (http://www.enzolifesciences.com/BML-2836/screenwell-epigenetics-library/). Human ES/iPS cells were treated with each compound (10 μM) for 24 h. The H3K27 methylation levels, *OCT3/4* expression levels and cell viability were examined.

Electroporation

AAVS1, *c/EBPα*, *FOXA2*, *GSC*, *HHEX*, *HNF1α*, *HNF4α*, *HNF6*, *IFNαR1*, *IPS-1*, *RIG1* and *SOX17* loci were targeted using the donor plasmids and CRISPR/Cas9 plasmids (or TALEN plasmids). The human ES cells were treated with 10 μM VPA for 24 h. Human ES/iPS cells ($2.0 \times 1\ 0^6$ cells) were dissociated into single cells by using Accutase, and resuspended in the prewarmed Nucleofector Solution (Lonza). The electroporation was performed by using 4D-Nucleofector System and 4D-Nucleofector Kit (P3) (both from Lonza) according to the manufacturer's instructions. The ratio of Nucleofector Solution to the plasmid solution is 90 μl: 10 μl (total 100 μl). The plasmid solution consists of 5 μg donor plasmids, 5 μg CRISPR/Cas9 plasmids (or TALEN plasmids) and 1 μg RAD51-expressing plasmids. After the electroporation, the cells were seeded onto LN511-E8 (Nippi)-coated dishes, and cultured with the medium containing 10 μM ROCK inhibitor. After culturing for 2 days, the medium was replaced with 10 μM puromycin- and 5 μM GCV-containing medium. Note that a high concentration of puromycin is required for efficient homozygous targeted gene editing. Puromycin- and GCV-containing medium was replaced with the medium 48 h after its addition. After 10 days from the electroporation, 24 individual colonies were picked up and then seeded onto an LN511-E8-coated 24-well plate. After most of the wells became nearly confluent, PCR and sequencing analysis were performed to examine whether the clones were correctly targeted.

RESULTS

Low biallelic gene editing efficiency in a transcriptionally inactive gene

In this study, we aimed to develop a method to accomplish highly efficient homozygous targeted gene editing of human ES/iPS cells regardless of the target gene's transcriptional activity. We designed donor plasmids targeting a transcriptionally active gene, *AAVS1*, or transcriptionally inactive gene, *hepatocyte nuclear factor 4 alpha* (*HNF4α*) (Figure 1A). In undifferentiated human ES cells, the methylation levels of H3K27 in the *HNF4α* locus were higher than those in the *AAVS1* locus, while the methylation levels of H3K4 and acetylation levels of H3K27 in the *HNF4α* locus were lower than those in the *AAVS1* locus (Figure 1B). These results suggest that the *AAVS1* gene is located in transcriptionally active euchromatin, while the *HNF4α* gene is located in transcriptionally inactive heterochromatin. *AAVS1* was targeted by using a donor plasmid expressing the enhanced green fluorescent protein and puromycin-resistant (PuroR) protein under the control of the exogenous elongation factor 1 alpha (EF1α) promoter (Figure 1C, Supplementary Figure S1A). *HNF4α* was targeted by using a donor plasmid expressing the PuroR protein under the control of the exogenous EF1α promoter (Figure 1D, Supplementary Figure S1C). The EF1α–PuroR cassette was designed to replace the second exon of *HNF4α* to generate *HNF4α*-knockout human ES/iPS cells. Human ES/iPS cells were electroporated only with donor plasmids targeting *AAVS1* or *HNF4α*, and then PCR analyses were performed to examine whether single cell-derived human ES/iPS cells carry the transgene cassette at the targeted locus (Figure 1E and F). Without using TALEN or CRISPR/Cas9 plasmids, biallelically-targeted clones were not obtained in either gene (Supplementary Figure S1B and D). To enhance the HR efficiency of human ES/iPS cells, we used TALEN or CRISPR/Cas9 plasmids, which could induce the DNA DSB at the middle point of two homology arms (Supplementary Figures S2A and B). When using the TALEN or CRISPR/Cas9 plasmids, 30% (7/24) of obtained clones carried the transgene at least one allele of *AAVS1* (Supplementary Figure S2C), while 4 (1/24)–8% (2/24) of obtained clones carried the transgene at least one allele of *HNF4α* (Supplementary Figure S2E). Notably, there were only a few clones (4–8%) that showed transgene integration into both alleles of *AAVS1*, but no clones which showed transgene integration into both alleles of *HNF4α*. A larger number of colonies was obtained by using CRISPR/Cas9 plasmids as compared with TALEN plasmids (Supplementary Figure S2D and F). We also confirmed that TALEN and CRISPR/Cas9 systems have similar activity in a fluorescent reporter assay using pCAG-EGxxFP (Supplementary Figures S2G and H). The genome cleavage activities of CRISPR/Cas9 system are also confirmed in Supplementary Figure S3E.

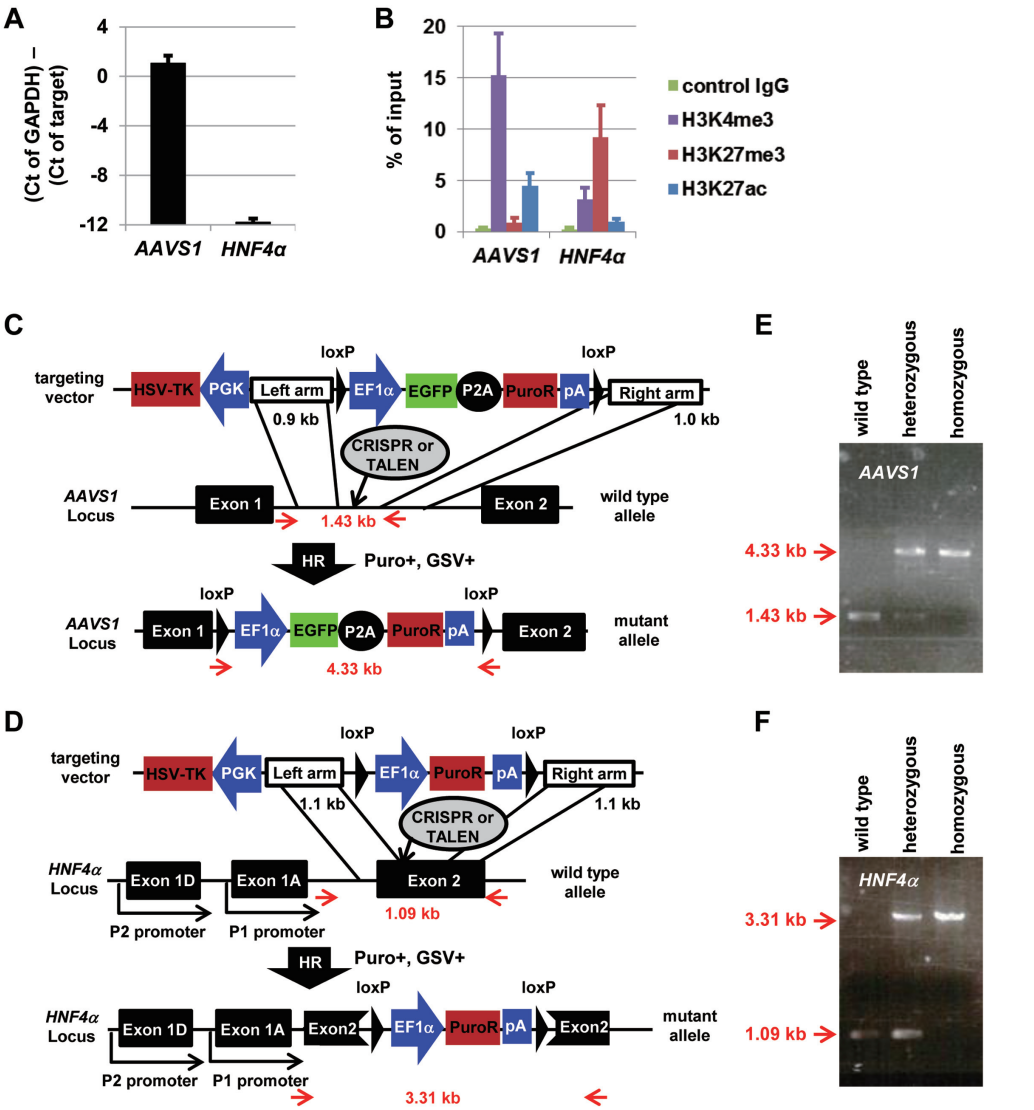

G

target gene	GSV	analyzed colony	no integration	random integration	correctly targeted clones: heterozygous obtained colony	heterozygous efficiency %	homozygous obtained colony	homozygous efficiency %
AAVS1	—	24	8	11	4	17	1	4
AAVS1	+	24	8	5	9	38	2	8
HNF4α	—	24	4	18	2	8	0	0
HNF4α	+	24	4	15	5	21	0	0

Figure 1. Low efficiency of biallelic gene editing in a transcriptionally inactive gene. (**A**) The gene expression levels of *GAPDH*, *adeno-associated virus integration site 1* (*AAVS1*) and *hepatocyte nuclear factor 4 alpha* (*HNF4α*) in human ES cells were examined by real-time RT-PCR analysis. (**B**) The H3K4me3, H3K27me3 and H3K27ac modification levels in the designed arm region of *AAVS1* and *HNF4α* loci were examined by ChIP-qPCR analysis. Data represent mean ± SEM of three independent experiments (Figure 1A and B). (**C** and **D**) The schematic overview shows the targeting strategy for (C) *AAVS1* and (D) *HNF4α*. PCR primers which can distinguish wild type and mutant alleles are shown with red arrows. Indicated targeting plasmids were used to target the *AAVS1* and *HNF4α* loci, respectively. Donor plasmids: EF1α; elongation factor 1 alpha promoter, EGFP; enhanced green fluorescent protein, P2A; self-cleaving P2A peptide sequence, PuroR; puromycin resistant protein, pA; polyadenylation sequence, PGK; phosphoglycerate kinase promoter, HSV-TK; herpesvirus thymidine kinase gene. The CRISPR/Cas9 and TALEN system were applied to produce *AAVS1* or *HNF4α* sequence-specific double-strand breaks (DSBs) (the details are described in Supplementary Figure S2A or S2B, respectively). (**E** and **F**) The PCR products obtained from the wild type, heterozygous and homozygous clones are shown. To confirm the DNA sequence, the PCR products were purified and subjected to sequencing analysis. (**G**) *AAVS1* or *HNF4α* loci were targeted using the donor plasmids and CRISPR/Cas9 plasmids. Human ES cells (H9) were electroporated with the donor plasmids and CRISPR/Cas9 plasmids. After the electroporation, the cells were seeded onto LN511-E8-coated dishes, and cultured with medium containing ROCK inhibitor. After culturing for 2 days, the medium was replaced with the puromycin- and GCV-containing medium. The puromycin- and GCV-containing medium was replaced with the medium 48 h after its addition. After 10 days from the electroporation, 24 individual colonies were picked up, and then seeded onto an LN511-E8-coated 24-well plate. After most of the wells became nearly confluent, PCR and sequencing analyses were performed to examine whether the clones were correctly targeted. Data represent a representative experiment of two independent experiments.

Although the HR efficiency of human ES/iPS cells was improved by using TALEN or CRISPR/Cas9 plasmids, the transgene was randomly integrated into chromosomes in most of the obtained clones or there was no integration. In particular, 91.7 (22/24)–95.8% (23/24) of the obtained clones were not correctly integrated into the *HNF4α* locus, but rather were randomly integrated into the chromosomes or were not integrated anywhere (Supplementary Figure S2E). This result suggests that TALEN or CRISPR/Cas9 systems might increase the potential risk of random integration. To improve the relative targeting efficiency, the herpes virus thymidine kinase gene was also encoded in the donor plasmids (Figure 1C and D). The human ES/iPS cells were electroporated with donor plasmids and CRISPR/Cas9 plasmids, and then subjected to positive selection with puromycin and negative selection with ganciclovir (GSV). The targeting efficiency in both *AAVS1* and *HNF4α* loci was increased by GSV treatment (Figure 1G). However, no clones showed transgene integration into both alleles of *HNF4α*, although two clones did have transgene integration into both alleles of *AAVS1*. Taken together, these results showed that the HR efficiency of human ES/iPS cells could be enhanced by using TALEN- or CRISPR/Cas9-mediated DSB and GSV-mediated negative selection. Nevertheless, the HR efficiency was not high enough to integrate the transgene into both alleles of a transcriptionally inactive gene such as *HNF4α*.

RAD51 overexpression increased the biallelic HR efficiency

To integrate the transgene into both alleles of a transcriptionally inactive gene, such as *HNF4α*, the enhancement of the HR efficiency is necessary. It is known that there is a large difference in HR efficiency among the mammalian cells (9). We also confirmed that there was an inter-human ES/iPS cell line difference in the HR efficiency (Figure 2A). To identify the key factor that plays an important role in the HR, we searched for HR-related genes which were highly correlated with the HR efficiency in human ES/iPS cells (Figure 2B). The global gene expression profiles were examined in six human ES/iPS cells lines. The top three HR-related genes (PPP4R2, CHEK1 and RAD51), the expression levels of which were correlated with the HR efficiency in human ES/iPS cells, are shown in Figure 2C. To examine whether these three genes could enhance the HR efficiency, human ES/iPS cells were co-transfected with HR-related gene (PPP4R2, CHEK1 or RAD51)-expressing plasmids, donor plasmids and CRISPR/Cas9 plasmids (Figure 2D). Importantly, the HR efficiency in the *AAVS1* locus was enhanced approximately 2.5-fold by RAD51 overexpression. Although no clones showed transgene integration into both alleles of the transcriptionally inactive gene, *HNF4α*, in the control group, 8% (2/24) of the obtained clones were biallelically targeted by RAD51 overexpression. We also confirmed that RAD51 accumulation in the *AAVS1* and *HNF4α* loci was promoted by RAD51 overexpression (Figure 2E and F, respectively). Importantly, the RAD51/X-ray repair cross complementing 4 (XRCC4) ratio in the *AAVS1* and *HNF4α* loci was also enhanced by RAD51 overexpression. Because XRCC4 is an essential component of NHEJ, it is suggested that HR might occur in higher probability than NHEJ. Taken together, these results indicated that the efficiency of CRISPR/Cas9-induced biallelic-targeted gene editing could be increased by RAD51 overexpression through enhancement of RAD51 accumulation in the targeted locus.

VPA treatment increased the biallelic HR efficiency

To further improve the efficiency of CRISPR/Cas9-induced biallelic-gene editing, we considered that a factor that could transiently loosen nucleosome folding of transcriptionally inactive chromatin might have potential to enhance the HR efficiency. It is widely known that histones can be modified with epigenetic marks that influence chromatin structure, and the methylation of the lysine residue 27 of histone H3 (H3K27) is an important epigenetic mark that is closely linked with transcriptional repression. It is also known that small-molecule compound screening is an effective experimental approach to accurately regulate cellular behavior such as direct reprogramming and survival of human ES/iPS cells (12–15). Therefore, a small-molecule compound screening using an epigenetics library was performed to identify a molecule that could transiently loosen the nucleosome folding of transcriptionally inactive chromatin without negatively affecting the pluripotency of human ES/iPS cells. A summary of the small-molecule compound screening is given in Figure 3A. For the first screening, the methylation levels of the H3K27 in the *HNF4α* locus were examined. ChIP-qPCR analysis showed that the 29 of the 43 compounds examined could decrease the methylation levels of H3K27 (Figure 3B, Supplementary Figure S3A). For the second screening, the gene expression levels of *OCT3/4* were examined because it is known that a critical amount of *OCT3/4* is required to sustain stem-cell self-renewal, and alteration of the expression levels of this gene induces the differentiation process (16). qPCR analysis showed that 17 of the 29 compounds tested did not largely alter the OCT3/4 expression levels (inducing a 0.5- to 2.0-fold change) (Figure 3C, Supplementary Figure S3B). For the third screening, the cell viability was examined. A WST-8 assay showed that valproic acid (VPA), valproic acid hydroxamate (VPAH) and butyrolactone 3 were the top three compounds in terms of preserving the cell viability (Figure 3D, Supplementary Figure S3C). To examine whether these three compounds could improve the efficiency of CRISPR/Cas9-induced biallelic gene editing, human ES/iPS cells were pre-treated with VPA, VPAH or butyrolactone 3 for 24 h, and then electroporated with donor plasmids and CRISPR/Cas9 plasmids (Figure 3E). The HR efficiency in the *AAVS1* locus was enhanced ∼2-fold by VPA or VPAH treatments. Although no clones showed transgene integration into both alleles of the transcriptionally inactive gene, *HNF4α*, in the control groups, 4 (1/24)–8% (2/24) of the obtained clones were homozygously targeted by VPA or VPAH treatment. These results indicated that the efficiency of CRISPR/Cas9-induced biallelic gene editing could be increased by VPA treatment.

To examine the mechanism of enhancement of biallelic HR efficiency by VPA treatment, we first examined the expression level of HDAC because VPA is known as a HDAC inhibitor. Among several HDACs, the protein expression

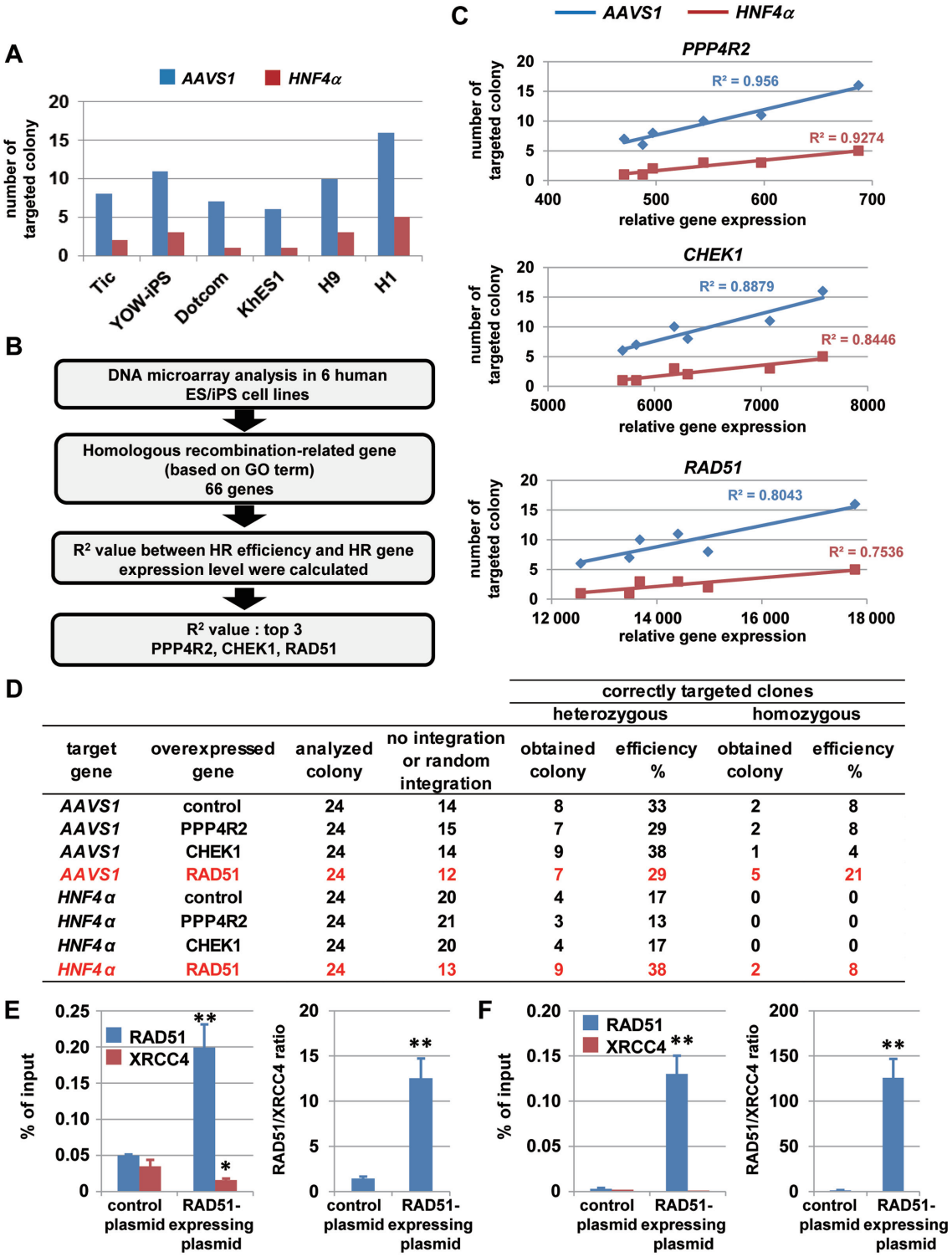

target gene	overexpressed gene	analyzed colony	no integration or random integration	correctly targeted clones: heterozygous obtained colony	heterozygous efficiency %	homozygous obtained colony	homozygous efficiency %
AAVS1	control	24	14	8	33	2	8
AAVS1	PPP4R2	24	15	7	29	2	8
AAVS1	CHEK1	24	14	9	38	1	4
AAVS1	RAD51	24	12	7	29	5	21
HNF4α	control	24	20	4	17	0	0
HNF4α	PPP4R2	24	21	3	13	0	0
HNF4α	CHEK1	24	20	4	17	0	0
HNF4α	RAD51	24	13	9	38	2	8

Figure 2. RAD51 overexpression increased the biallelic targeting efficiency in human ES/iPS cells. (**A**) Six human ES/iPS cell lines were electroporated with the donor plasmids (for *AAVS1* and *HNF4α*) and CRISPR/Cas9 plasmids. Then, 24 colonies were analyzed by PCR to examine whether they were homozygously or heterozygously targeted. Data represent a representative experiment of two independent experiments. (**B**) The experimental outline of the HR-related factor screening is shown. (**C**) R^2 values between the number of correctly targeted colonies and relative gene expression levels (*PPP4R2*, *CHEK1* or *RAD51*) are shown. Data represent a representative experiment of two independent experiments. (**D**) Human ES cells (H9) were electroporated with the donor plasmids, CRISPR/Cas9 plasmids and PPP4R2-, CHEK1- or RAD51-expressing plasmids. PCR analysis was performed to examine whether the clones were correctly targeted. Data represent a representative experiment of two independent experiments. (**E** and **F**) Human ES cells were electroporated with the donor plasmids, CRISPR/Cas9 plasmids and RAD51-expressing plasmids. The RAD51 and XRCC4 recruitment levels around the gRNA-targeting sequence in (E) *AAVS1* and (F) *HNF4α* loci were examined by ChIP-qPCR analysis. The RAD51/XRCC4 recruitment ratio was also calculated. Data represent mean ± SEM of three independent experiments. $^*P < 0.05$, $^{**}P < 0.01$ (compared with control plasmid).

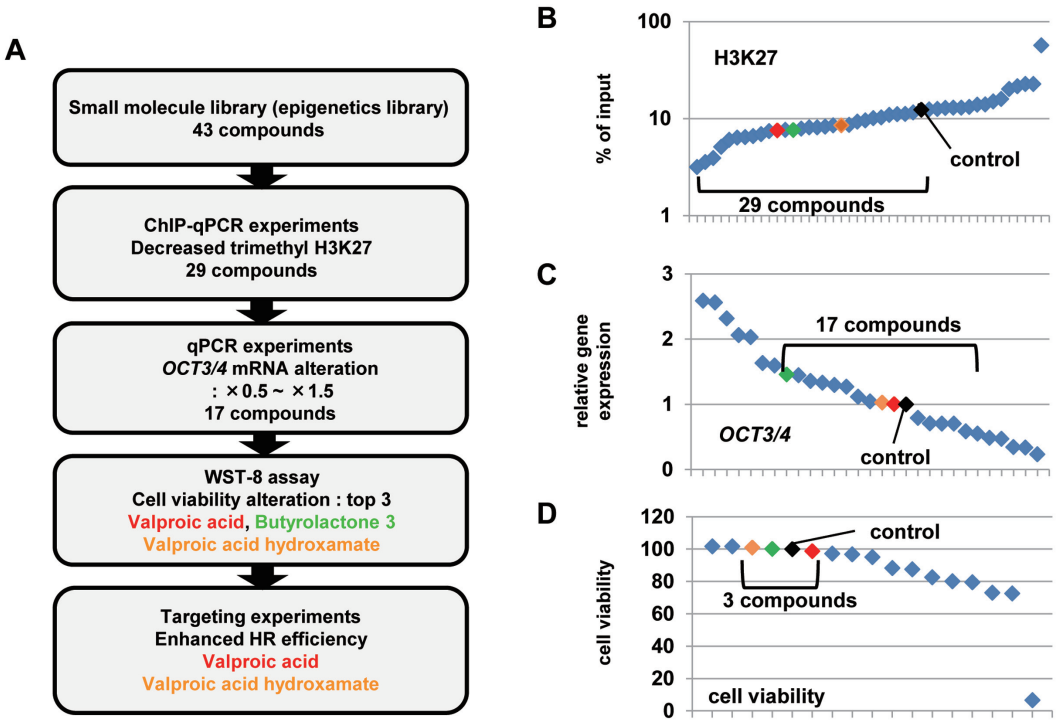

E

target gene	treated compound	analyzed colony	no integration or random integration	correctly targeted clones: heterozygous obtained colony	heterozygous efficiency %	homozygous obtained colony	homozygous efficiency %
AAVS1	control	24	15	7	29	2	8
AAVS1	VPA	24	11	8	33	5	21
AAVS1	VPAH	24	11	9	38	4	17
AAVS1	BL3	24	16	7	29	1	4
HNF4α	control	24	21	3	13	0	0
HNF4α	VPA	24	14	8	33	2	8
HNF4α	VPAH	24	15	8	33	1	4
HNF4α	BL3	24	22	2	8	0	0

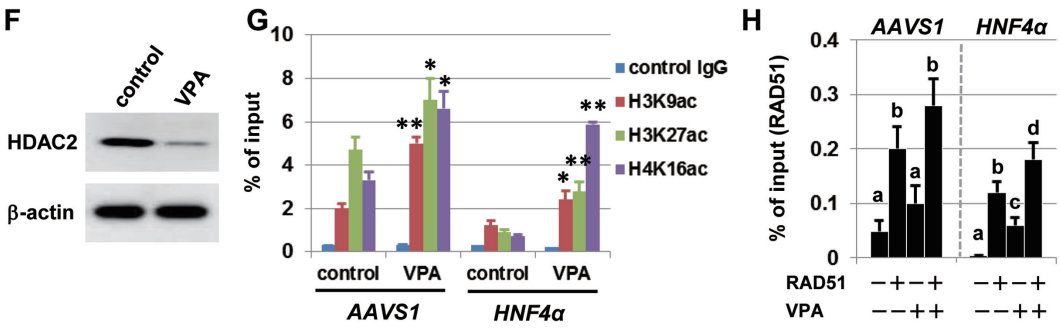

Figure 3. Valproic acid (VPA) treatment increased the biallelic targeting efficiency in human ES/iPS cells. (**A**) The experimental outline of the small-molecule compound screening is shown. (**B**) The human ES cells (H9) were treated with 43 small molecules (10 μM) for 24 h. The tri-methylation levels of H3K27 in the designed arm region of the *HNF4α* locus were examined by ChIP-qPCR analysis. (**C**) The gene expression levels of *OCT3/4* were examined by real-time RT-PCR analysis. The gene expression levels in the DMSO-treated cells were taken as 1.0. (**D**) The cell viability was assessed by WST-8 assay. The cell viability in the DMSO-treated cells was taken as 100. Data represent a representative experiment of two independent experiments (Figure 3B–D). (**E**) The human ES cells were treated with VPA, VPAH or butyrolactone 3 (BL3) for 24 h, and then were electroporated with the donor plasmids and CRISPR/Cas9 plasmids. PCR analysis was performed to examine whether the clones were correctly targeted. Data represent a representative experiment of two independent experiments. (**F**) The protein expression level of HDAC2 in VPA-treated human ES cells was examined by western blotting. Data represent a representative experiment of two independent experiments. (**G**) The H3K9ac, H3K27ac and H4K16ac modification levels in the designed arm region of *AAVS1* and *HNF4α* loci were examined by ChIP-qPCR analysis. $*P < 0.05$, $**P < 0.01$ (compared with control). (**H**) The RAD51 recruitment levels around the gRNA-targeting sequence in *AAVS1* and *HNF4α* loci were examined by ChIP-qPCR analysis. Data represent mean ± SEM of three independent experiments (Figure 3G and H). Groups that do not share the same letter are significantly different from each other ($P < 0.05$).

level of HDAC2 in human ES cells was decreased by VPA treatment (Figure 3F). Importantly, the acetylation levels of H3K9, H3K27 and H4K16 in the *AAVS1* and *HNF4α* loci were significantly increased by VPA treatment (Figure 3G). In addition, RAD51 recruitment in the targeted locus was promoted by VPA treatment (Figure 3H). We confirmed that the expression levels of RAD51, Cas9 and Fok1 were not changed by VPA treatment (Supplementary Figure S3D). In addition, the efficiency of DSB by CRISPR/Cas9 was not change by RAD51 overexpression and VPA treatment (Supplementary Figure S3E). Moreover, the expression levels of targeted genes (*AAVS1* and *HNF4α*) (Supplementary Figure S3F), expression levels of pluripotent markers (Supplementary Figure S3G) and differentiation potency (Supplementary Figure S4E) were not changed by RAD51 overexpression and VPA treatment. Taken together, these results showed that VPA treatment could enhance the efficiency of biallelic genome editing by loosening the nucleosome folding of transcriptionally inactive chromatin without changing nuclease activities, pluripotent state or differentiation capacity. A detailed characterization of established human ES/iPS cells (GFP-expressing human ES cells and HNF4α-knockout human ES cells) is presented in Supplementary Figures S4 and S5, respectively.

RAD51 overexpression and VPA treatment synergistically increased the biallelic HR efficiency

We expected that the HR efficiency would be further enhanced by combining RAD51 overexpression and VPA treatment. And indeed, the HR efficiency in cells receiving both treatments was higher than that in cells receiving only RAD51 overexpression or only VPA treatment (Figure 4A). This result was confirmed in *AAVS1* gene and three transcriptionally inactive genes, *HNF4α*, *FOXA2* and *IPS-1*. These results also indicate that the number of randomly integrated colonies and not-integrated colonies could decrease by using our method. In addition, the HR efficiency was not largely affected by the length of the inserted cassette (Supplementary Figure S6). We also confirmed that the HR efficiency could be enhanced by RAD51 overexpression and VPA treatment in *c/EBPα*, *FOXA2*, *GSC*, *HHEX*, *HNF1α*, *HNF4α*, *HNF6*, *IFNαR1*, *IPS-1*, *RIG1* and *SOX17* loci (Figure 4B). Furthermore, similar results could be obtained in human mesenchymal stem cells as well as human ES/iPS cells (Supplementary Figure S7). More than 20% of the obtained colonies were homozygously targeted in both the transcriptionally active and inactive genes. These results indicated that RAD51 overexpression and VPA treatment synergistically increased the HR efficiency. Figure 4C summarizes the established protocol for highly efficient CRISPR/TALEN-mediated homozygous targeted gene editing in human ES/iPS cells by RAD51 overexpression and VPA treatment.

Low incidence of off-target effects in CRISPR-mediated homozygous targeting with RAD51 overexpression and VPA treatment

To examine the off-target effect of CRISPR-mediated homozygous targeting with RAD51 overexpression and VPA treatment, karyotype analysis, comparative genomic hybridization analysis and exome sequencing were performed. Almost all of the parental human iPS cells (wild-type cells; WT) and homozygous targeted human iPS cells (HNF4α-knockout cells; HNF4α-KO) showed normal karyotypes (Figure 5A and B). We also confirmed that there were no large genomic deletion or insertion except the *HNF4α* locus we targeted (Figure 5C). In addition, we performed exome sequencing to examine whether genomic mutations had occurred by using CRISPR-mediated homozygous targeting with RAD51 overexpression and VPA treatment (Figure 5D). Importantly, there were no additional mutations in the potential off-target sites that were predicted by sequence similarity-up to five mismatches-with the on-target site (Supplementary Table S1). In addition, the frequency of random integration, which occurs in addition to the desired targeting events, was not enhanced by RAD51 overexpression and VPA treatment (Supplementary Figure S5E and F). These results suggest that there was a low incidence of off-target effects in our homozygous targeting method. However, we only analyzed exome which does not cover the majority of the human genome and we did not analyze sequence similarity-up to more than six mismatches-with the on-target site. Further analysis, such as GUIDE-seq analysis (17), might be needed in the future.

DISCUSSION

In this study we found that RAD51 overexpression and VPA treatment synergistically increased the biallelic HR efficiency regardless of the transcriptional activity of the targeted locus. We confirmed our finding in 12 loci, *AAVS1*, *c/EBPα*, *FOXA2*, *GSC*, *HHEX*, *HNF1α*, *HNF4α*, *HNF6*, *IFNαR1*, *IPS-1*, *RIG1* and *SOX17* loci. RAD51 is a molecule that plays an important role in the HR of DNA during DSB repair (18). Vispe *et al*. have reported that 2- to 3-fold overexpression of the RAD51 protein stimulated a 20-fold increase in HR efficiency in CHO cells (19). It is also reported that the *in vitro* application of an HDR enhancer, RS-1, which stimulates RAD51 expression, increases the knock-in efficiency (20,21). Consistently, RAD51 overexpression could also increase HR efficiency in human ES/iPS cells (Figure 2D). It is known that DSBs are repaired by NHEJ and HR. The ratio of RAD51 (key regulator of HR) to XRCC4 (key regulator of NHEJ) in the targeted locus was enhanced by RAD51 overexpression (Figure 2E and F). These results suggest that the efficiency of HR after the CRISPR/TALEN-mediated DSBs would be enhanced by RAD51 overexpression.

It is known that VPA has a negative effect on HDAC (22). Previously, Defoort *et al*. have also demonstrated that VPA treatment could increase the HR frequency in CHO cells (23). Consistently, we confirmed that VPA treatment decreased HDAC2 expression level (Figure 3F). Importantly, we found that VPA treatment could increase the acetylation levels of H3K9, H3K27 and H4K16 at both the transcriptionally active and inactive loci without affecting the characteristics of human ES/iPS cells (Figure 3G). Therefore, these facts suggest that VPA treatment enhanced CRISPR/TALEN-mediated HR efficiency in hu-

A

target gene	treatment	analyzed colony	no integration or random integration	correctly targeted clones: heterozygous obtained colony	heterozygous efficiency %	homozygous obtained colony	homozygous efficiency %
AAVS1	control	24	14	8	33	2	8
AAVS1	VPA	24	11	8	33	5	21
AAVS1	Rad51	24	12	7	29	5	21
AAVS1	VPA + RAD51	24	2	13	54	9	38
HNF4α	control	24	21	3	13	0	0
HNF4α	VPA	24	15	8	33	1	4
HNF4α	RAD51	24	13	9	38	2	8
HNF4α	VPA + RAD51	24	3	15	63	6	25
FOXA2	control	24	20	4	17	0	0
FOXA2	VPA	24	13	9	38	2	8
FOXA2	Rad51	24	12	9	38	3	13
FOXA2	VPA + RAD51	24	2	14	58	8	33
IPS-1	control	24	19	5	21	0	0
IPS-1	VPA	24	10	11	46	3	13
IPS-1	RAD51	24	11	11	46	2	8
IPS-1	VPA + RAD51	24	3	12	50	9	38

B

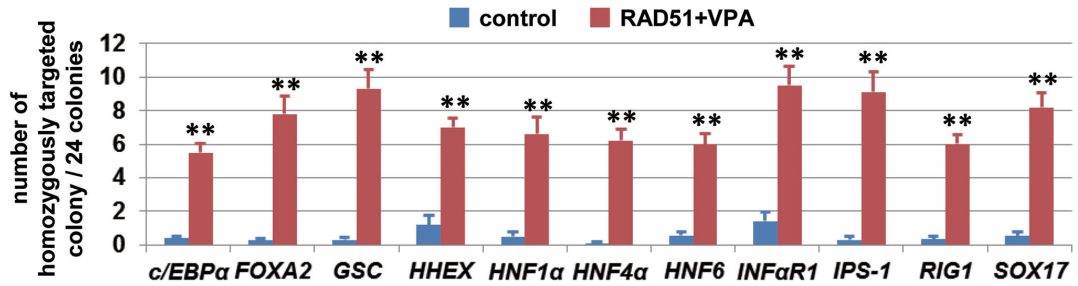

C

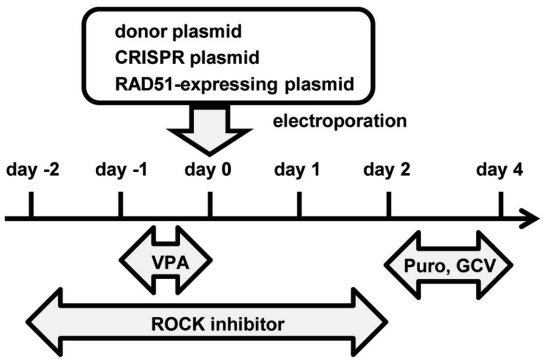

Figure 4. Synergistical effect of RAD51 and VPA. (**A**) The human ES cells (H9) were treated with 10 μM VPA for 24 h, and were electroporated with the donor plasmids, CRISPR/Cas9 plasmids and RAD51-expressing plasmids for *AAVS1*, *HNF4α*, *FOXA2* and *IPS-1*. PCR analysis was performed to examine whether the clones were correctly targeted. Data represent a representative experiment of two independent experiments. (**B**) The human ES cells were treated with 10 μM VPA for 24 h, and were electroporated with the donor plasmids, CRISPR/Cas9 plasmids and RAD51-expressing plasmids for *c/EBPα*, *FOXA2*, *GSC*, *HHEX*, *HNF1α*, *HNF4α*, *HNF6*, *IFNαR1*, *IPS-1*, *RIG1* and *SOX17*. PCR analysis was performed to examine whether the clones were correctly targeted. Data represent mean ± SEM of three independent experiments. $^{**}P < 0.01$ (compared with control). (**C**) The established protocol for efficient biallelic-targeted gene editing in human ES/iPS cells by RAD51 overexpression and VPA treatment is summarized.

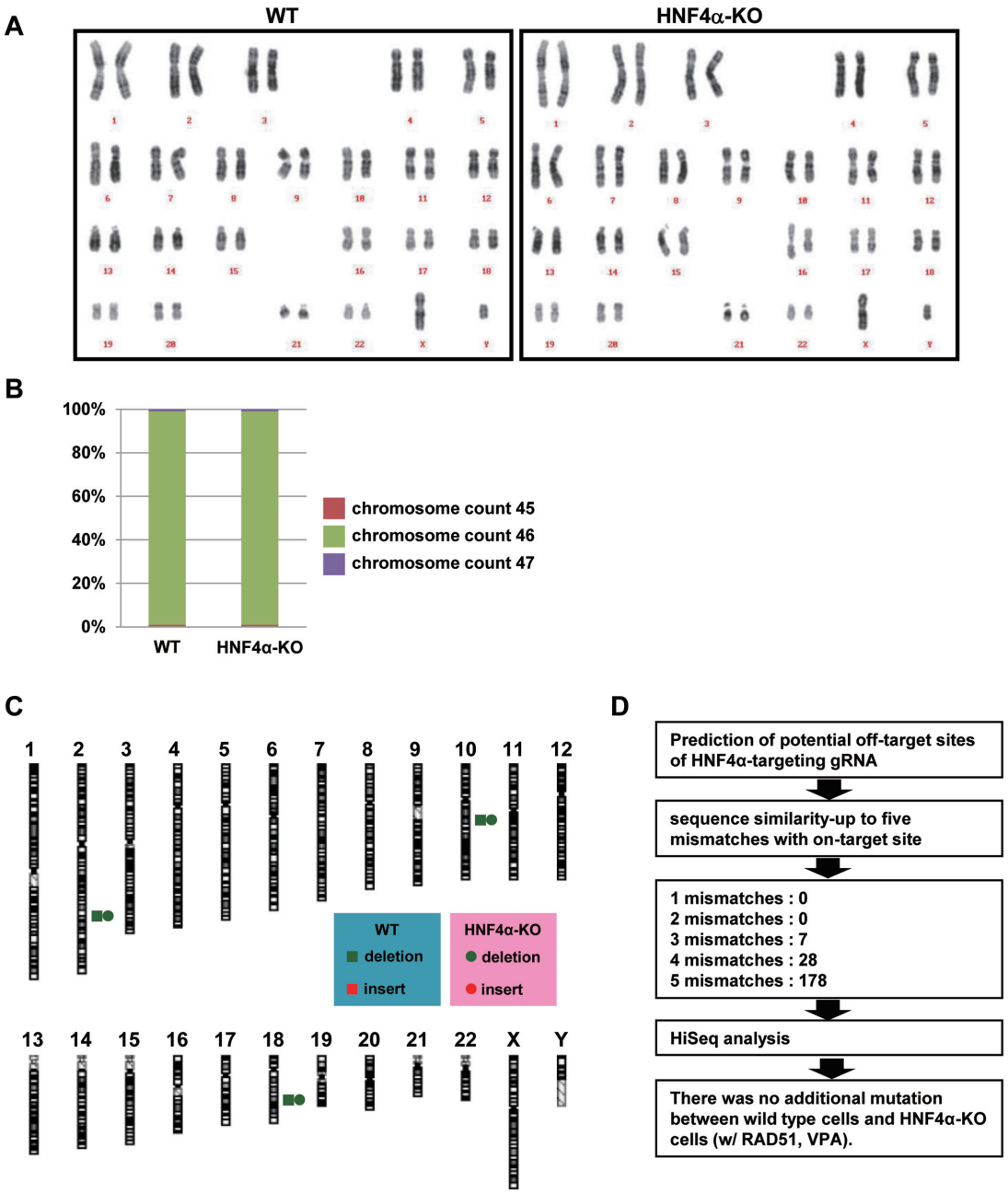

Figure 5. Off-target effect of RAD51 and VPA. (**A**) Karyotypes of human iPS cells (YOW-iPS) and HNF4α-knockout human iPS cells are shown. Chromosomal Q-band analyses showed that both cells had a normal karyotype, indicating that the genetic stability of human iPS cells was confirmed throughout the HR process by our method. (**B**) Karyotype and (**C**) comparative genomic hybridization analysis was performed in the parental human iPS cells (wild-type cells; WT) and homozygous targeted human iPS cells (HNF4α-knockout cells; HNF4α-KO). Data represent a representative experiment of two independent experiments. (**D**) Exome sequencing was performed in wild-type cells and HNF4α-knockout cells. Genomic sequences of the potential off-target sites, which were predicted by sequence similarity-up to five mismatches-with on-target site, were examined.

man ES/iPS cells because VPA treatment loosened nucleosome folding in transcriptionally inactive chromatin.

Because our biallelic gene editing method using a RAD51-expressing plasmid and small molecule, VPA, is simple and effective, we believe that it would be broadly applicable to various field researches that use human ES/iPS cells. However, RAD51 overexpression and VPA treatment could not increase the NHEJ efficiency in human ES/iPS cells. Therefore, it was suggested that the mechanism of NHEJ in human ES/iPS cells is largely different from that of HR. Our findings will facilitate the genome editing research in human ES/iPS cells irrespective of the transcriptional activity of the targeted locus.

SUPPLEMENTARY DATA

Supplementary Data are available at NAR Online.

ACKNOWLEDGEMENTS

The authors thank Ms. Ayaka Sakamoto and Ms. Natsumi Mimura for her excellent technical support. The authors also thank Dr Masato Ikawa (Osaka University) for helpful discussion. pENTR donor plasmid was kindly provided from Dr Akitsu Hotta (Center for iPS Cell Research and Application, Kyoto University). The authors also thank Dr Eiri Ono (K-CONNEX, Kyoto University) for his drawing of Graphical abstract.

FUNDING

Japan Society for the Promotion of Science (JSPS) KAKENHI [10759509]; Keihanshin Consortium for Fostering the Next Generation of Global Leaders in Research (K-CONNEX), established by Human Resource Development Program for Science and Technology, MEXT; Japan Agency for Medical Research and development, AMED [15fk0210002h0002, 15bk0104005h0003].
Conflict of interest statement. None declared.

REFERENCES

1. Gaj,T., Gersbach,C.A. and Barbas,C.F. 3rd (2013) ZFN, TALEN, and CRISPR/Cas-based methods for genome engineering. *Trends Biotechnol.*, **31**, 397–405.
2. Sakuma,T. and Woltjen,K. (2014) Nuclease-mediated genome editing: At the front-line of functional genomics technology. *Dev. Growth Differ.*, **56**, 2–13.
3. Smith,C., Gore,A., Yan,W., Abalde-Atristain,L., Li,Z., He,C., Wang,Y., Brodsky,R.A., Zhang,K., Cheng,L. *et al.* (2014) Whole-genome sequencing analysis reveals high specificity of CRISPR/Cas9 and TALEN-based genome editing in human iPSCs. *Cell Stem Cell*, **15**, 12–13.
4. Veres,A., Gosis,B.S., Ding,Q., Collins,R., Ragavendran,A., Brand,H., Erdin,S., Cowan,C.A., Talkowski,M.E. and Musunuru,K. (2014) Low incidence of off-target mutations in individual CRISPR-Cas9 and TALEN targeted human stem cell clones detected by whole-genome sequencing. *Cell Stem Cell*, **15**, 27–30.
5. Ding,Q., Lee,Y.K., Schaefer,E.A., Peters,D.T., Veres,A., Kim,K., Kuperwasser,N., Motola,D.L., Meissner,T.B., Hendriks,W.T. *et al.* (2013) A TALEN genome-editing system for generating human stem cell-based disease models. *Cell Stem Cell*, **12**, 238–251.
6. Ding,Q., Regan,S.N., Xia,Y., Oostrom,L.A., Cowan,C.A. and Musunuru,K. (2013) Enhanced efficiency of human pluripotent stem cell genome editing through replacing TALENs with CRISPRs. *Cell Stem Cell*, **12**, 393–394.
7. Hockemeyer,D., Soldner,F., Beard,C., Gao,Q., Mitalipova,M., DeKelver,R.C., Katibah,G.E., Amora,R., Boydston,E.A., Zeitler,B. *et al.* (2009) Efficient targeting of expressed and silent genes in human ESCs and iPSCs using zinc-finger nucleases. *Nat. Biotechnol.*, **27**, 851–857.
8. Hockemeyer,D., Wang,H., Kiani,S., Lai,C.S., Gao,Q., Cassady,J.P., Cost,G.J., Zhang,L., Santiago,Y., Miller,J.C. *et al.* (2011) Genetic engineering of human pluripotent cells using TALE nucleases. *Nat. Biotechnol.*, **29**, 731–734.
9. Yu,C., Liu,Y., Ma,T., Liu,K., Xu,S., Zhang,Y., Liu,H., La Russa,M., Ding,S. *et al.* (2015) Small molecules enhance CRISPR genome editing in pluripotent stem cells. *Cell Stem Cell*, **16**, 142–147.
10. Chu,V.T., Weber,T., Wefers,B., Wurst,W., Sander,S., Rajewsky,K. and Kuhn,R. (2015) Increasing the efficiency of homology-directed repair for CRISPR-Cas9-induced precise gene editing in mammalian cells. *Nat. Biotechnol.*, **33**, 543–548.
11. Kawabata,K., Sakurai,F., Yamaguchi,T., Hayakawa,T. and Mizuguchi,H. (2005) Efficient gene transfer into mouse embryonic stem cells with adenovirus vectors. *Mol. Ther.*, **12**, 547–554.
12. Zhu,S., Rezvani,M., Harbell,J., Mattis,A.N., Wolfe,A.R., Benet,L.Z., Willenbring,H. and Ding,S. (2014) Mouse liver repopulation with hepatocytes generated from human fibroblasts. *Nature*, **508**, 93–97.
13. Wang,H., Cao,N., Spencer,C.I., Nie,B., Ma,T., Xu,T., Zhang,Y., Wang,X., Srivastava,D. and Ding,S. (2014) Small molecules enable cardiac reprogramming of mouse fibroblasts with a single factor, Oct4. *Cell Rep.*, **6**, 951–960.
14. Li,K., Zhu,S., Russ,H.A., Xu,S., Xu,T., Zhang,Y., Ma,T., Hebrok,M. and Ding,S. (2014) Small molecules facilitate the reprogramming of mouse fibroblasts into pancreatic lineages. *Cell Stem Cell*, **14**, 228–236.
15. Watanabe,K., Ueno,M., Kamiya,D., Nishiyama,A., Matsumura,M., Wataya,T., Takahashi,J.B., Nishikawa,S., Muguruma,K. and Sasai,Y. (2007) A ROCK inhibitor permits survival of dissociated human embryonic stem cells. *Nat. Biotechnol.*, **25**, 681–686.
16. Niwa,H., Miyazaki,J. and Smith,A.G. (2000) Quantitative expression of Oct-3/4 defines differentiation, dedifferentiation or self-renewal of ES cells. *Nat. Genet.*, **24**, 372–376.
17. Tsai,S.Q., Zheng,Z., Nguyen,N.T., Liebers,M., Topkar,V.V., Thapar,V., Wyvekens,N., Khayter,C., Iafrate,A.J., Le,L.P. *et al.* (2015) GUIDE-seq enables genome-wide profiling of off-target cleavage by CRISPR-Cas nucleases. *Nat. Biotechnol.*, **33**, 187–197.
18. Baumann,P. and West,S.C. (1998) Role of the human RAD51 protein in homologous recombination and double-stranded-break repair. *Trends Biochem. Sci.*, **23**, 247–251.
19. Vispe,S., Cazaux,C., Lesca,C. and Defais,M. (1998) Overexpression of Rad51 protein stimulates homologous recombination and increases resistance of mammalian cells to ionizing radiation. *Nucleic Acids Res.*, **26**, 2859–2864.
20. Pinder,J., Salsman,J. and Dellaire,G. (2015) Nuclear domain 'knock-in' screen for the evaluation and identification of small molecule enhancers of CRISPR-based genome editing. *Nucleic Acids Res.*, **43**, 9379–9392.
21. Song,J., Yang,D., Xu,J., Zhu,T., Chen,Y.E. and Zhang,J. (2016) RS-1 enhances CRISPR/Cas9- and TALEN-mediated knock-in efficiency. *Nat. Commun.*, **7**, 10548.
22. Gottlicher,M., Minucci,S., Zhu,P., Kramer,O.H., Schimpf,A., Giavara,S., Sleeman,J.P., Lo Coco,F., Nervi,C., Pelicci,P.G. *et al.* (2001) Valproic acid defines a novel class of HDAC inhibitors inducing differentiation of transformed cells. *EMBO J.*, **20**, 6969–6978.
23. Defoort,E.N., Kim,P.M. and Winn,L.M. (2006) Valproic acid increases conservative homologous recombination frequency and reactive oxygen species formation: a potential mechanism for valproic acid-induced neural tube defects. *Mol. Pharmacol.*, **69**, 1304–1310.